UNITED STATES DEPARTMENT OF THE INTERIOR
GEOLOGICAL SURVEY

FIELD INVESTIGATION TO IDENTIFY A SITE FOR MONITORING LIQUEFACTION, CHOLAME VALLEY, CALIFORNIA

Thomas L. Holzer[1], Michael J. Bennett[1], T. Leslie Youd[2], and Albert T.F. Chen[1]

Open-File Report
86-346

[1]USGS, Menlo Park, California [2]Brigham Young University, Utah

1986

CONTENTS

page

ILLUSTRATIONS

TABLES

APPENDICES

ABSTRACT

Standard penetration and cone penetration tests were conducted in the Cholame Valley to find a sand deposit that would liquefy during the predicted (1988) Parkfield earthquake ($M_L \approx 5.6$). Tests indicate that the upper 1-m of a lenticular sand deposit between depths of 5.1 and 11.5 m will liquefy during the Parkfield earthquake. The location of the sand deposit is 2 km south of Cholame Ranch and 0.7 km west of the San Andreas fault. Instrumentation of the liquefiable sand provides an excellent opportunity to measure and record the build-up and dissipation of pore-water pressure that would accompany the predicted earthquake.

Introduction

This report presents results from a subsurface investigation to find a site suitable for monitoring pore-water pressure changes in sediment undergoing earthquake-induced liquefaction. The sand at the proposed site is to be monitored with piezometers and accelerometers. The investigation was conducted in Cholame Valley, California (fig. 1), where a moderate ($M_L \approx 5.6$) earthquake is anticipated before 1993 and where sediment has liquefied in previous earthquakes.

Continuous records of earthquake-induced strong-ground motion and resulting pore-water pressure changes are needed to improve our understanding of liquefaction under field conditions and to test theoretical models of liquefaction (Committee on Earthquake Engineering, 1985). The proposed site in the Cholame Valley would be the fifth operational site established for the purpose of measuring seismically induced pore-water pressure. The other sites are in the Imperial Valley, California, on St. Helens Mtn., Washington (2), and on Owi Island in Tokyo Bay, Japan. Todate, only the Owi Island site has recorded earthquake-induced residual pore-water pressure changes. On September 25, 1980, a magnitude 6.1 earthquake with a peak ground acceleration of 0.097 g generated residual pore-water pressures at depths of 6 and 14 m correspond to 19 and 16 percent of the effective overburden pressure, respectively (Ishihara and others, 1981).

Liquefaction During Previous Earthquakes

Liquefaction in Cholame Valley has been induced by previous earthquakes. The only comprehensive post-earthquake field investigation was conducted after the last moderate earthquake ($M_L \approx 5.6$) on June 27, 1966 (Brown and others, 1967). Evidence of liquefaction was found at three locations where small surficial sand and silt deposits were formed by ejection of water (fig. 1). In addition, unverified reports of water spouts were reported a few kilometers southeast of Cholame Ranch where the active fault trace steps across the valley and in the general area of the proposed instrumentation site. Liquefaction also may have contributed to some of the embankment failures along Cholame Creek north of Highway 46 (see Brown and others, 1967, Fig. 35).

Liquefaction probably has occurred in pre-1966 earthquakes but documentation is poor. Brown and others (1967, p. 9-10) summarized publications and interviews with local residents that describe ground failures associated with these earthquakes.

Regional Geology and Seismology

Structural Geology and Seismolgy

Cholame Valley is a small rift valley within the San Andreas fault zone. Although the fault zone has a maximum width of 2 km in Cholame Valley, surficial faulting in 1966 was restricted to two parallel traces (Brown and others (1966) and fig. 1). The longer trace can be followed southward for 29 km along the northeast side of the valley until approximately 3.5 km south of Cholame Ranch where it steps over to the southwest side of the valley and continues for an additional 9 km. Brown and others (1967) considered this trace to be the main active trace of the San Andreas fault. The other trace is in the northern part of the valley on its southwest side. The fault on this side is discontinuous and trends parallel to the main trace for about 8 km (fig. 1).

The Cholame Valley segment of the San Andreas fault zone is one of the most historically active segments of the 950-km long fault (Brown and others, 1967). Bakun and McEvilly (1984) have proposed that five moderate earthquakes have occurred along the segment since 1857. The last moderate earthquake was on June 27, 1966, when the valley was shaken by a $M_L \approx 5.6$ earthquake. The mean recurrence interval of the five earthquakes is 21.9 years and the standard deviation of the mean is only 3.1 years (Bakun and Lindh, 1985). Bakun and McEvilly (1984) reevaluated seismograph reocrds of the last three moderate earthquakes in 1922, 1934, and 1966 and concluded that these earthquakes had nearly identical source parameters (epicenter location, magnitude, seismic moment, source area, and unilateral southeast-rupture propagation). They also inferred that the two pre-instrumental earthquakes in 1881 and 1901 were similar to the last three earthquakes. These authors proposed that there is a characteristic Parkfield earthquake with local and moment magnitudes of about 5.6 and 6.0, respectively, and a recurrence interval of 22 years. They proposed that the next characteristic Parkfield earthquake will happen in early 1988. The estimated 95 percent confidence interval for the predicted date is 1988.0 ± 5.2 years (Bakun and Lindh, 1985).

Peak horizontal accelerations associated with the characteristic Parkfield earthquake can be estimated on the basis of recordings from the 1966 Parkfield earthquake and the general attentuation of peak acceleration with distance observed during earthquakes in California. Five accelerograms within 16-km of the south end of the surface rupture were obtained during the 1966 earthquake (Cloud and Perez, 1967). Peak accelerations of about 0.5 g were recorded on the two accelerometers closest to the surface rupture. The two instruments were 82 m and 5.31 km from the rupture. The 0.5 g acceleration compares favorably with the peak-horizontal acceleration inferred from strong-ground motion attentuation curves observed from other earthquakes in California (Joyner and Boore, 1981). Most of the earthquakes were associated with strike-slip events. The 50 and 84 percentile values of peak-horizontal acceleration within about 4-km of the surface rupture for moment magnitude 6.0 events are 0.4 and 0.7 g, respectively.

Stratigraphy

The San Andreas fault zone divides Cholame Valley into two tectonic blocks (Dibblee, 1973). Bedrock of the eastern block consists of Franciscan Formation sedimentary and igneous rocks. Bedrock of the western block consists of granitic and metamorphic rock. Both of these blocks are overlain by consolidated marine sedimentary rocks and the Plio-Pleistocene Paso Robles Formation.

Cholame Valley is underlain by unconsolidated sediment with a thickness that may locally exceed 200 m. The valley fill consists of clay, silt, sand, and gravel that originated in alluvial, fluvial, and possibly lacustrine environments. Variations in thickness and stratigraphy of the valley fill are poorly known from driller's logs and geophysical traverses.

The valley fill beneath the area south of Cholame Ranch, where we concentrated our investigation, appears to consist of a thick sequence of predominatly fine-grained sediment. Owners of the land in this area indicated that test wells in the valley fill penetrated as much as 240 m of unconsolidated "blue clay". The presence of the "blue clay" at shallow depth was confirmed by our exploratory drilling. Undisturbed samples of blue clayey silt were retrieved from 23.3 m, and the deposit can be inferred to extend to

a depth of at least 30 m on the basis of cone penetration testing. A 42-m section of blue silty clay also was logged in the upper part of an exploratory borehole at the south end of the valley (R.E. Warrick, written communication, 1985).

Exploration Strategy, Methods, and Results

Exploration Strategy

Our exploration program focussed on finding a site with the following attributes: (1) a shallow water table, (2) a loose Holocene sand less than 15-m deep, and (3) proximity to the active trace of the San Andreas fault. The reasons for emphasizing these attributes were as follows. First, theoretical considerations indicate that susceptibility to liquefaction decreases as the depth to the water table increases. Second, experience in other earthquakes indicates that geologically youthful sandy alluvial deposits within 15 m of the land surface are the most susceptible to liquefaction. And third, most liquefaction caused by earthquakes smaller than magnitude 6.0 is restricted to within a few kilometers of the surface rupture.

Our investigation consisted of three phases- areal reconnaissance, cone penetration testing, and standard penetration testing- that were increasingly more site specific with each phase. The areal reconnaissance included hand augering near sites of 1966 liquefaction and seismic refraction profiling. The reconnaissance quickly targeted an area south of Cholame Ranch as the most likely location of a site with the desired attributes.

Areal Reconnaissance

Initial field reconnaissance in Cholame Valley consisted of surficial inspections and shallow hand-augered borings at locations where liquefaction was reported in 1966. Boreholes were augered to 2- to 3-m below the ground surface except the northermost liquefaction location where cobbly stream bed deposits prevented augering. Each hole was logged and water tables were measured in the open holes (appendix A). The reconnaissance indicated that the most promising area for finding a suitable site was about 1.5 km south of Cholame Ranch. In this area, Cholame Creek changes abruptly from an incised stream to a braided stream and appears to be presently depositing most of its bedload. The area also had a shallow water table in January 1985, typically the driest month of the year.

Subsequently, nine 65-m-long seismic-refraction lines were occuppied south of Cholame Ranch (figs. 1 and 2) to determine the thicknesses and seismic velocities of the shallow deposits. Lines were oriented paralled to the axis of the valley. Results from all but one of the lines were interpreted by horizontal two-layer models (appendix B). The P-wave velocities of the upper and lower layers averaged 350 and 1480 m/s, respectively. Depths to the top of the 1480 m/s layer ranged from less than 0.9 to 7.3 m (appendix B). The one exception, SR-3, to the two-layer model may have encountered a third layer with a velocity of about 3650 m/s at a depth of about 21 m.

The 1480 m/s velocity compares favorably with the velocity of the valley fill determined by R. E. Warrick (written communication, 1985) near the south end of Cholame Valley (fig. 1). Warrick's velocities were also measured by seismic refraction but he used explosives and a wider geophone spacing that precluded detection of the upper layer found in our investigation. Velocities

of the upper layer in Warrick's investigation ranged from 1600 to 1900 m/s, whereas the underlying material had a velocity greater than 3100 m/s.

Depth to water from the land surface at the seismic refraction lines ranged from 0.8 to 3.4 m in early June 1985 (appendix C). The water table was shallowest, 1.0 to 1.5 m, in the area near the dry bed of Cholame Creek beginning 1.5 km south of Cholame Ranch.

Cone Penetration Test (CPT)

Three profiles south of Cholame Ranch were established with 20 CPT soundings (fig.2). Sounding depths ranged from 16.7 to 30.7 m. Profiles A (fig. 3) and B (fig. 4), are perpendicular to the axis of the valley. Profile C (fig. 5), is parallel to the valley axis near Cholame Creek. The sounding at CPT A6 encountered the thickest, 6.4-m, sand layer between depths of 5.1 and 11.5 m (fig. 3). Subsequent soundings were made to determine the lateral extent of the sand layer.

The CPT measures the penetration resistance of a right-angle cylinder with a conical tip as it is pushed into the soil. Resistance is measured every 5 cm at both the tip of the cone and along a sleeve located behind the cone. The cone used in this investigation was a 10-cm^2 substraction cone (Robertson and Campanella, 1984) that used compression-type load cells to measure resistance. Procedures and equipment were consistent with the requirements of ASTM D3441-79.

Although no samples are obtained with the CPT, the resistance characteristics of sand and clay make them readily distinguishable. Cohesionless soil can be recognized by high tip resistance (q_c) values and low ratios of sleeve (f_s) to tip resistance (less than two percent). The ratio of sleeve resistance to tip resistance is referred to as the friction ratio (R_f). Cohesive soil has low tip resistance values and high friction ratios (greater than four percent).

Standard Penetration Test (SPT)

Standard penetration tests were conducted at CPT A5, A6, A7, C2, and C3 where the shallow saturated sand layer identified by the CPT soundings was thickest. Blow counts and the CPT profile at CPT A6 are shown in figure 6.

The SPT measures the penetration resistance of a sampling spoon driven one foot into the soil by a special hammer. The SPT method compensates for two disadvantages of the CPT. First, the SPT obtains a sample that can be used to determine the lithology of the deposit. Second, investigations with the SPT have been conducted world-wide on deposits that have and have not liquefied during earthquakes. Correlations of these SPT results with observed strong-ground motions form the basis for a widely used technique for evaluating liquefaction resistance of sand (Seed and others, 1985).

The SPT procedure that was followed is outlined in ASTM D1586-67; modifications to the procedure are described by Youd and Bennett (1983). Holes were drilled using 6-in outside diameter, 2.5-in inside diameter, hollow-stem augers. The sampler used is a Mobile "ADO Standard Penetration Sampler" that is lined (constant inside diameter of 1 3/8 in). For each test the sampler was seated 6 inches into the soil and then the number of hammer blows for each of the next two 6-inch intervals was recorded; the total number of blows for the last foot of penetration is the standard penetration

resistance, N. The sampler was driven with a 140-lb Mobile "In-Hole Sampling Hammer" that was lifted and then dropped 30 in with a Mobile "Safe-T-Driver" hoist. The calibrated efficiency of the hammer is 68 percent of an ideal free-fall hammer (Douglas and Strutynsky, 1984).

Geotechnical Data

Samples collected during the SPT investigation were examined in the field for texture, stratification, and color (Munsell color chart, 1975). Water contents (ASTM D 2216-80), grain-size distributions (ASTM D 422-63) and Atterberg limits (ASTM D424-59 and D423-66) were determined in the laboratory.

Sediment was classified using both a ternary size diagram (fig. 7) and the Unified Soil Classification System (U.S. Army Corps of Engineers, 1953). Grain-size distributions and geotechnical data are shown in figure 8 and appendix D, respectively.

Two undisturbed samples from CPT A6 were obtained with thin-walled Shelby tubes for consolidation and permeability tests. Oedometer tests on sediment between a depth of 3.7 and 4.3 m indicated a preconsolidation pressure of 2.9 kg/cm^2 which yields an overconsolidation ratio of about 3. Sediment between 17.4 and 18.0 m had a preconsolidation pressure of 4.5 kg/cm^2 which yields an overconsolidation ratio of 1.3. These ratios suggest that the uppermost part of the sediment column may be overconsolidated, but that the sediment probably is normally consolidated between a depth of 5.1 and 18.0 m. The laboratory-determined vertical permeability of the clayey silt at a depth of 4 m was 1.25×10^{-4} cm/sec.

Interpretation and Analysis

Site Hydrogeology

The prospective instrument site near CPT A6 has a surprisingly shallow water table in view of the arid climate of Cholame Valley. Water tables in early June 1985 were all within about 2 m of the land surface. The high water-table condition also appears to be relatively constant throughout the year. Two standpipe piezometers at depths of 2.5 and 10 m and 1-m apart, were installed near CPT A6 during the SPT investigation in July 1985. Water-level differences in each piezometer between July and December 1985, which approximates the beginning and ending of the dry part of the year, were only 0.2 m (appendix C).

Our investigation was not sufficiently comprehensive either to determine the cause of or to assess the permanency of the shallow water table. Two possible sources of recharge to the shallow-water flow system were recognized, Cholame Creek and the ground-water system in bedrock.

The most obvious source of recharge is Cholame Creek. The stream is perennial, typically flowing only from about December to late spring. During field work in early June 1985, the stream was obviously recharging the ground-water system. The stream had significant discharge at Cholame Ranch but was dry near CPT A6. Local recharge is suggested by the configuration of the water table. The gradient of the water table in June, inferred from the hand-augered holes in the study area, was 0.4 percent and sloped southward away from the area of stream infiltration (Appendix C).

The other potential source of recharge is upward flow from the regional bedrock ground-water system. Such a possibility is suggested by free-flowing

wells that discharge from the valley fill in the study area. However, the two piezometers at CPT A6, which were completed at different depths, did not indicate a vertical-hydraulic gradient in either July or December. The shallow piezometer was screened near the base of the uppermost sand layer, unit A. The deep piezometer was screened near the base (11 m below the surface) of the thickest sand layer, unit C (fig. 6)

Site Stratigraphy and Environment of Deposition

The stratigraphy at CPT A6 is shown in figure 6. Four distinctive units were identified in the 30-m interval penetrated: unit A, a 2.1-m-thick sand; unit B, a 3.0-m-thick clayey silt; unit C, a 6.4-m-thick sand; and unit D, a clayey silt that extends from 11.5 m to the bottom of the boring at 30 m. Unit C was further divided into three subunits which from top to bottom are; C1 (5.1 to 5.7 m), dark-grayish brown, moderately sorted, loose, medium-grained sand (SP-SM), C2 (5.7 to 7.7 m), dark-grayish brown, poorly sorted, medium dense, medium-grained sand (SP-SM), C3 (7.7 to 11.5 m), dark brown, poorly sorted, medium dense, gravelly sand (SW-SM). Gravel up to 40-mm in diameter is found near the bottom of C3. Contacts in unit C are gradational between subunits and are sharp at the top and bottom of the unit. Two intercalated sandy subunits D1 and D2, which are 1.4- and 1.2-m thick respectively, were recognized in unit D.

Units A, B, C, and D can be correlated throughout most of the area explored with the CPT (figs. 3-5). Unit A has a constant thickness throughout the area whereas unit B thickens to the west near CPT A1. Unit C is thickest, 6.4 m, near CPT A6 and A7 and thins to 1.0 and 2.0 m near CPT A1 and A10, respectively.

Units A and C probably are fluvial deposits. Unit A is contiguous with the modern stream bottom, which is part of a braided fuvial environment. Unit C is texturally similar to unit A. The fine grain size, lateral continuity, and flatness of the valley floor suggest units B and D may be lacustrine.

Site Liquefaction Characterization

The liquefaction resistance at CPT A6 was evaluated with PETAL2 (Chen, 1986) on the basis of the following conditions. First, the design earthquake was the characteristic Parkfield earthquake which has a local magnitude of 5.6 and an assumed peak-horizontal acceleration of 0.4 g at CPT A6. Second, the water table was assumed to be 1.7-m deep which corresponds to the depth when the CPT and SPT were made. And third, subunits C2 and C3 and unit D were assumed to have saturated densities of 2.1 g/cm^3 (130 pcf); units A and B and subunit C1 were assumed to have densities of 1.9 g/cm^3 (120 pcf). Densities of the shallow unsaturated zone were treated as if it were saturated.

Grain-size distributions of unit A and C and subunits D1 and D2 indicate these layers may be susceptible to liquefaction (figs. 7 and 8). The analysis of liquefaction resistance thus focussed on these layers. The liquefaction resistance of unit A was not evaluated, however, because only its lower part remains saturated. The significant gravel and fine contents of units C and D (appendix D) complicates the analysis of their resistance to liquefaction. The liquefaction behavior of sediment that is both gravelly and silty is not well understood. Therefore, the effect of these components were treated separately.

Three approaches were used to estimate the liquefaction resistance of unit C and subunits D1 and D2. The first approach considered the deposits to be silty sand and ignored the effects of the gravel. In this approach blow counts were used to estimate liquefaction resistance according to the procedure of Seed and others (1985). The liquefaction resistance of silty sand as a function of normalized blow count is shown in figure 9. The SPT data used to calculate the liquefaction resistance are shown in table 1. The boundary curves that separate liquefaction from no liquefaction (fig. 9) were were modified from the standard 7.5 magnitude position to a position that corresponds to a 5.6 magnitude earthquake following the procedure of Seed and others (1985, p. 24). The second approach treated the units as gravelly sand with less than five percent fine content. It followed the same steps prescribed in the first approach but applied a correction for the gravel content (Ishihara, 1985). The correction factor as a function of gravel content is shown in figure 10. The third approach used Ishihara's (1985) method which determines the liquefaction resistance directly from tip resistance measured by the CPT (fig. 11). In this method the relation between liquefaction resistance and normalized tip resistance, q_c, is independent of earthquake magnitude. Corrections for gravel content are not considered in this method. The CPT data used to calculate the liquefaction resistance are shown in table 2.

Liquefaction resistance expressed in terms of the factor of safety against liquefaction is shown in table 3 for each of the three approaches. The factor of safety is the ratio of the cyclic-stress ratio required to liquefy a layer to the cyclic-stress ratio induced by the design earthquake. The cyclic-stress ratios themselves are shown in figure 12 as a function of depth. The results from the three approaches are consistent for unit C. The ratios indicate that subunit C1 and the upper part of C2 will liquefy during the characteristic Parkfield earthquake. Except for the base of unit C where the factor of safety is less than 1.2 the resistance to liquefaction in unit C generally increases with depth. Subunit D1 is marginally liquefiable by the SPT methods, but is marginally resistive by the CPT method. Subunit D2 is very resistive by the SPT methods and marginally resistive by the CPT method.

Conclusions

The area near CPT A6 in Cholame Valley, California, is underlain by a 1-m-thick loose sand layer that is capable of generating excess pore-water pressure equal to the overburden pressure if shaken by the characteristic Parkfield earthquake. The layer is the top part of 6.4-m-thick sand layer which extends from a depth of 5.1 m to 11.5 m. Vertical variations in the resistance to liquefaction within the 6.4-m-thick sand also offer the opportunity to investigate both the response of sand with a broad range of liquefaction resistances and the migration of pore pressures in a deposit undergoing liquefaction. The sand layer is overlain by a 3-m-thick clayey silt that probably will retard the decay of excess pore-water pressure.

The shallow water table at CPT A6 has remained relatively constant during 1985 and probably will not drop below 2 m. Thus, the liquefiable sand found at the site can be expected to be saturated when the characteristic earthquake occurs.

Acknowledgments

We are indebted to the Sunical Division of the Hearst Corporation, owner of Cholame Ranch and the property on which the exploration was conducted, for granting access to their property. Field expenses and exploration costs were supported by a contract to Brigham Young University from the Electric Power Research Institute. Drilling for the SPT investigations was conducted by Sam Shaler. Field assistance and laboratory tests were aprovided by Scott Hardman of Brigham Young University.

REFERENCES

Bakun, W.H., and Lindh, A.G., 1985, The Parkfield, California, earthquake prediction experiment: Science, v. 229, p. 619-624.

Bakun, W.H., and McEvilly, T.V., 1984, Recurrence models and Parkfield, California, earthqaukes: Journal of Geophysical Research, v. 89, no. B5, p. 3051-3058.

Brown, R.D.,Jr., Vedder, J.G., Wallace, R.E., Roth, E.F., Yerkes, R.F., Castle, R.O., Waananen, A.O., Page, R.W., and Eaton, J.P., 1967, The Parkfield-Cholame Earthquakes of June-August 1966--Surface geologic effects, water-resources aspects, and preliminary seismic data: U.S. Geological Survey Professional Paper 579, 66 p.

Chen, A.T.F., 1986, PETAL2, PEnetration Testing And Liquefaction, an interactive computer program: U.S. Geological Survey Open File Report 86-178, 31 p.

Cloud, W.K., and Perez, V., 1967, Accelerographs - Parfield earthquake: Seismological Society Bulletin, v. 57, no. 6, p. 1179-1192

Committee on Earthquake Engineering, 1985, Liquefaction of soils during earthquakes: Washington, D.C., National Academy Press, 240 p.

Dibblee, T.W., Jr., 1973, Stratigraphy of the southern Coast Ranges near the San Andreas fault from Cholme to Maricopa, California: U.S. Geological Survey Professional Paper 764, 45 p.

Douglas, B.J., and Strutynsky, A.I., 1984, Cone penetrometer test, pore pressure measurements and SPT hammer energy calibration for liquefaction hazard assessment: Earth Technology Corporation, Long Beach, California, U.S.G.S. Contract no. 14-08-001-19105.

Ishihara, K., 1985, Stability of natural deposits during earthquakes: Proceeding, 11th International Conference on Soil Mechanics and Foundation Engineering, San Francisco, California, v. 1,p. 321-376.

Ishihara, K., Shimizu, K., and Yamada, Y., 1981, Pore water pressures measured in sand deposits during an earthquake: Japanese Society of Soil Mechanics and Foundation Engineering, v. 21, no. 4, p. 85-100.

Joyner, W.B., and Boore, D.M., 1981, Peak horizontal acceleration and velocity from strong-motion records including records from the 1979 Imperial Valley, California, earthquake: Seismolgical Society of America Bulletin, v. 71, no. 6, p. 2011-2038.

Munsell Soil Color Chart, 1975, MacBeth Division of Kollmorgen Corporation, Baltimore, Maryland.

Robertson, P. K. and Campanella, R. G., 1984, Guidelines for use and interpretation of the electronic cone penetration test: Department of Civil Engineering, University of British Columbia, Vancouver, Cananda, Soil Mechanics Series no. 69

Seed, H.B., Tokimatsu, K., Harder, L.F., and Chung, R.M., 1985, Influence of SPT procedures in soil liquefaction resistance evaluations: American Society of Civil Engineers Journal of the Geotechnical Engineering Division, v. 111, no. 12, p. 1425-1445.

Tsuchida, H., 1970, Prediction and countermeasure against the liquefaction in sand deposits: Abstract of the Seminar in the Port and Harbor Research Institute, p. 3.1-3.33 (in Japanese).

Unified Soil Classification System, 1953, Technical Memorandum 3-357, U. S. Waterways Experiment Station, Vicksburg, Mississippi.

Youd, T.L., and Bennett, M.J., 1983, Liquefaction sites, Imperial Valley, California: American Society of Civil Engineers Journal of the Geotechnical Division, v. 109, no. 3, p. 440-457.

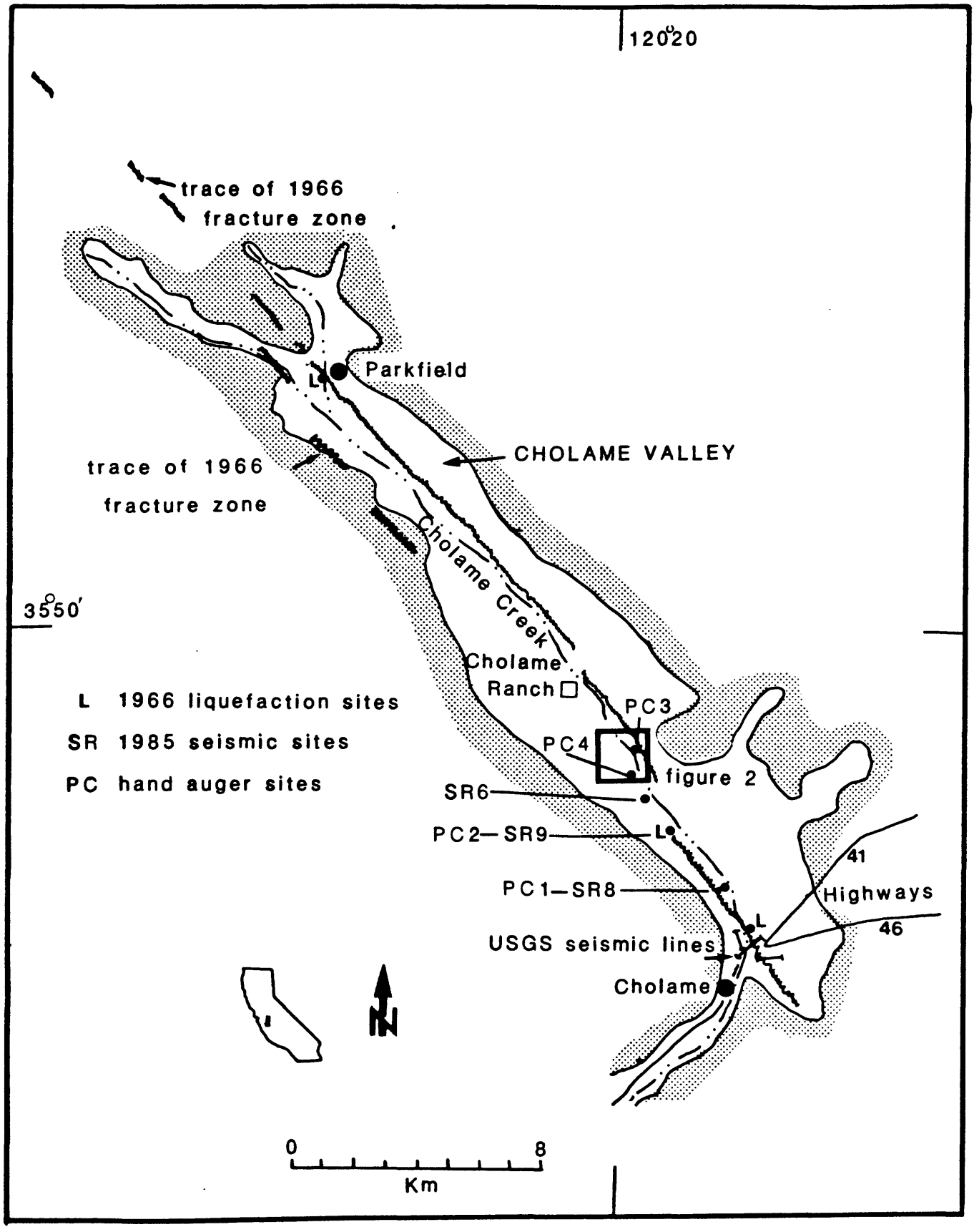

Figure 1. Location map, liquefaction sites and fault traces from Brown and others (1967).

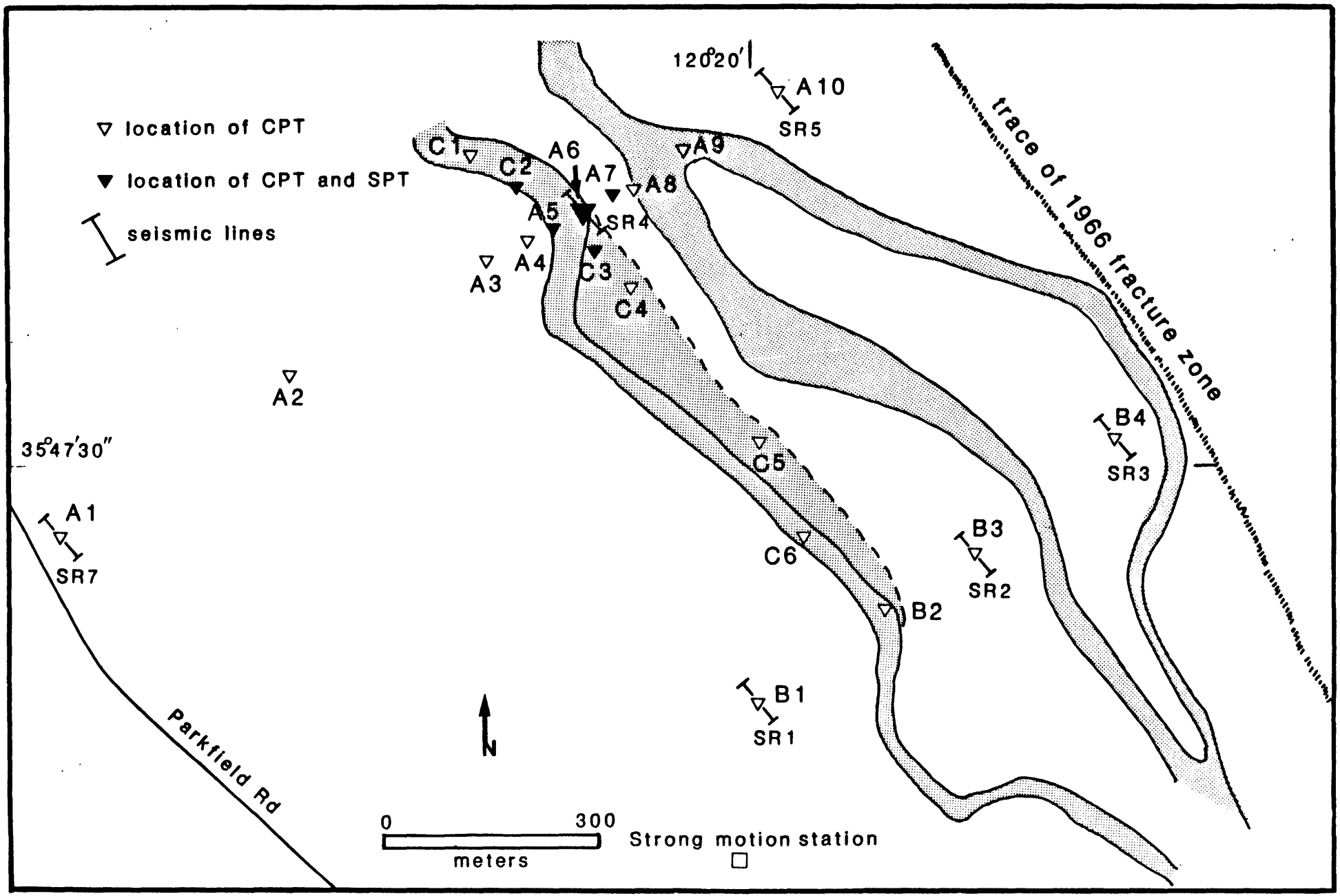

Figure 2. Map of study area. Stippled area with solid lines shows distribution of surface sand in 1978 (USGS 7.5' Cholame Valley Quadrangle map). Dashed line shows approximate distribtion of sand in 1985.

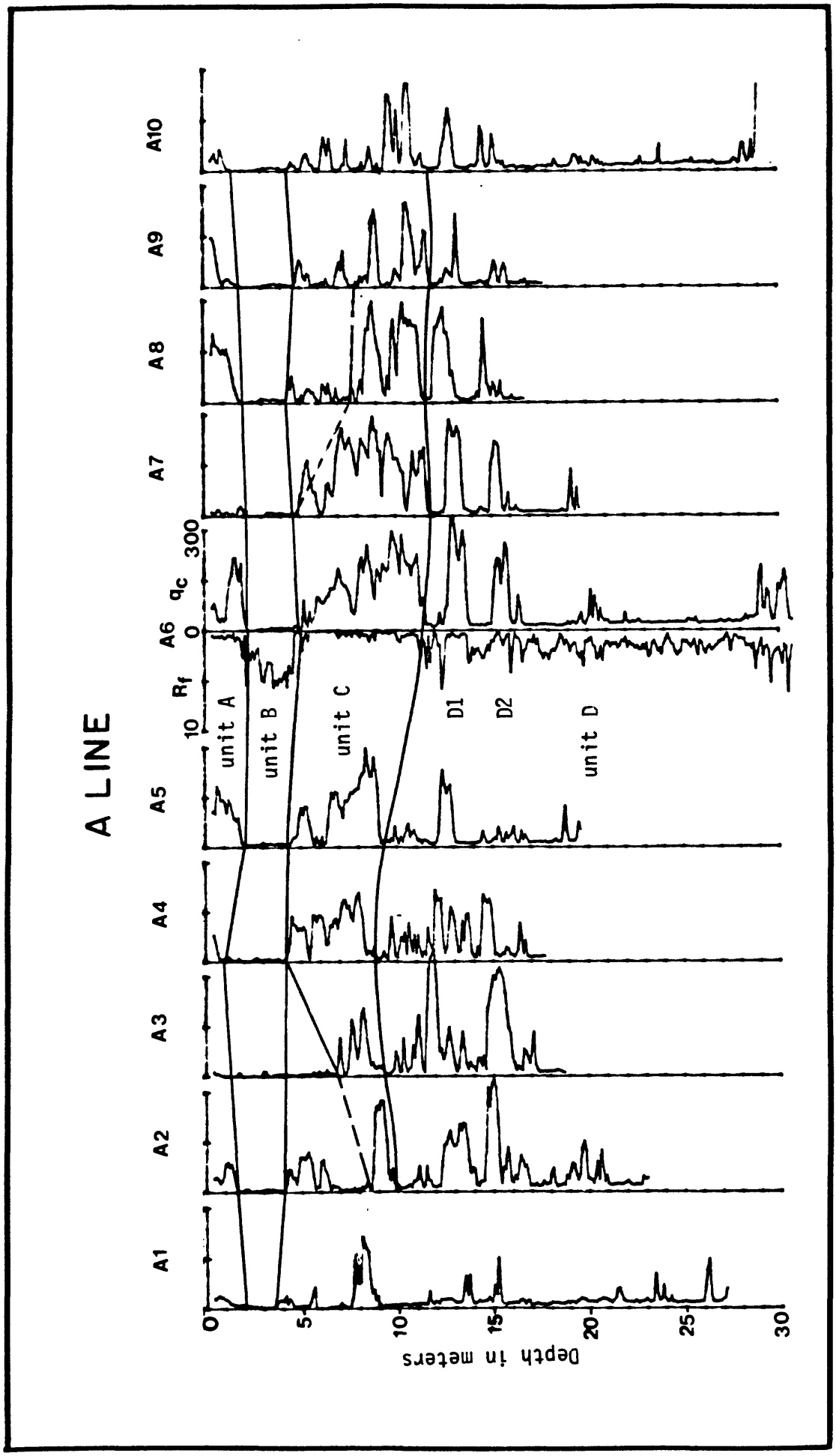

Figure 3. Cross section along A line, no horizontal scale. q_c is in kg/cm^2 and R_f is in percent.

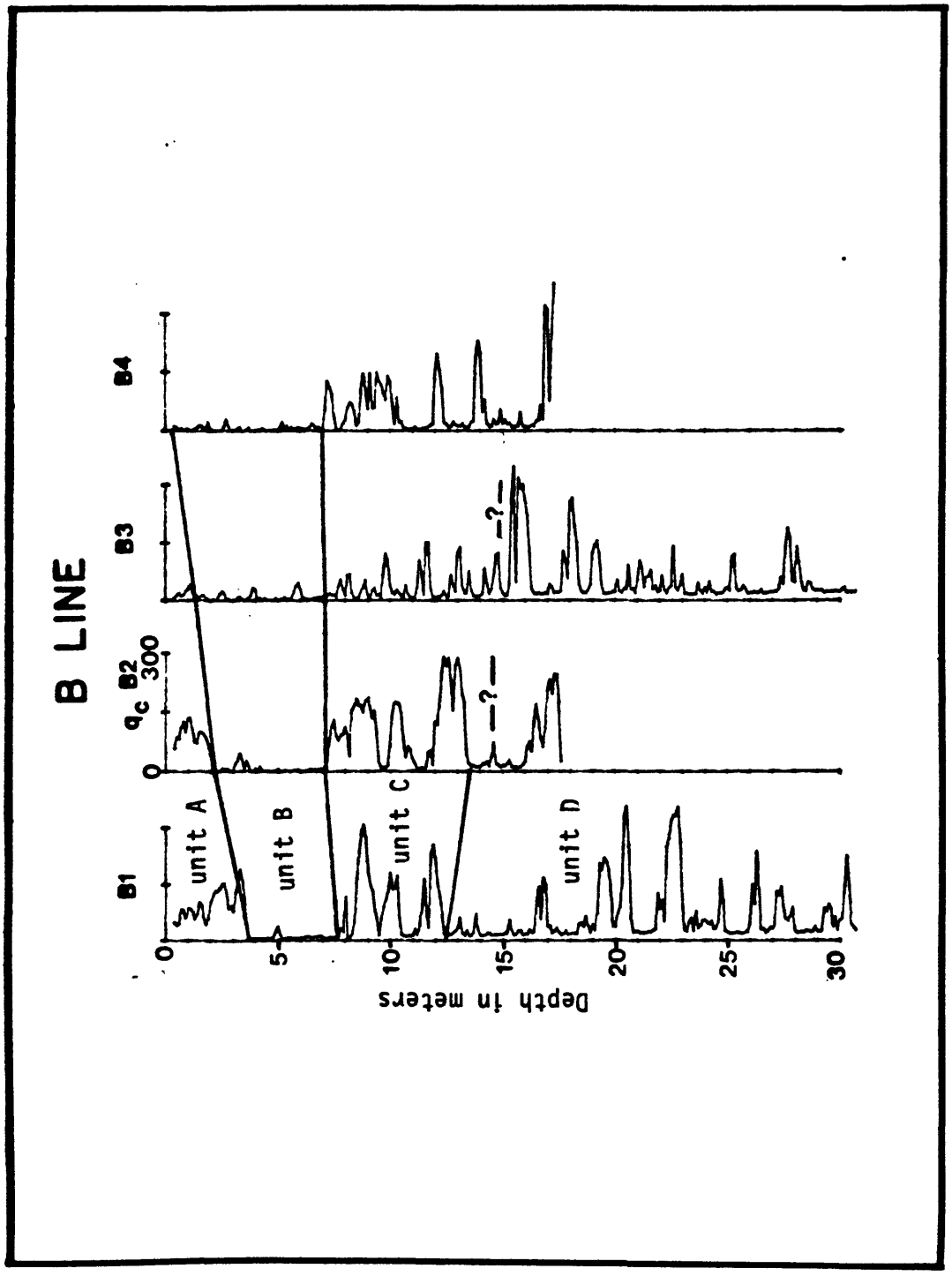

Figure 4. Cross section along B line, no horizontal scale. q_c is in kg/cm^2 and R_f is in percent.

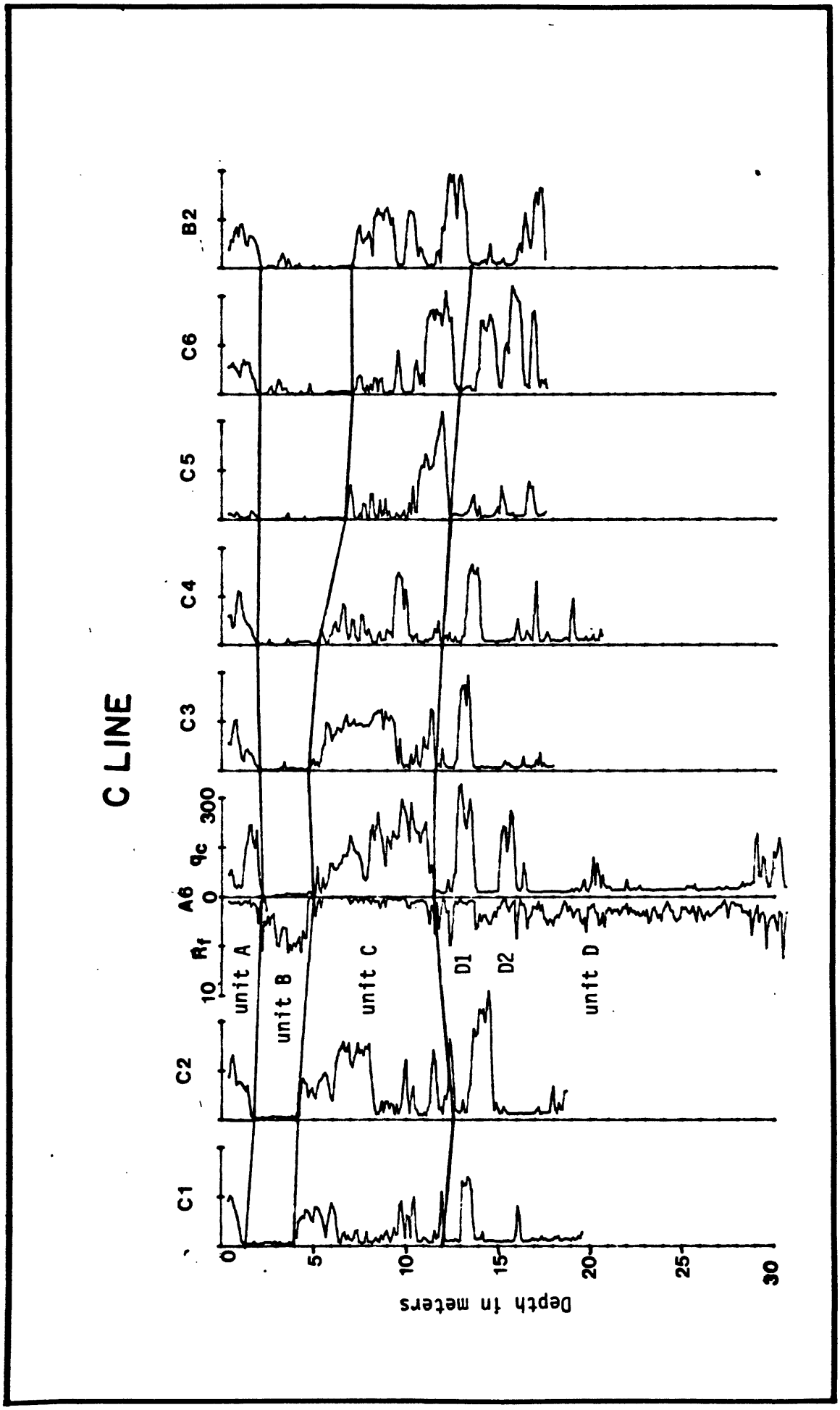

Figure 5. Cross section along C line, no horizontal scale. q_c is in kg/cm^2 and R_f is in percent.

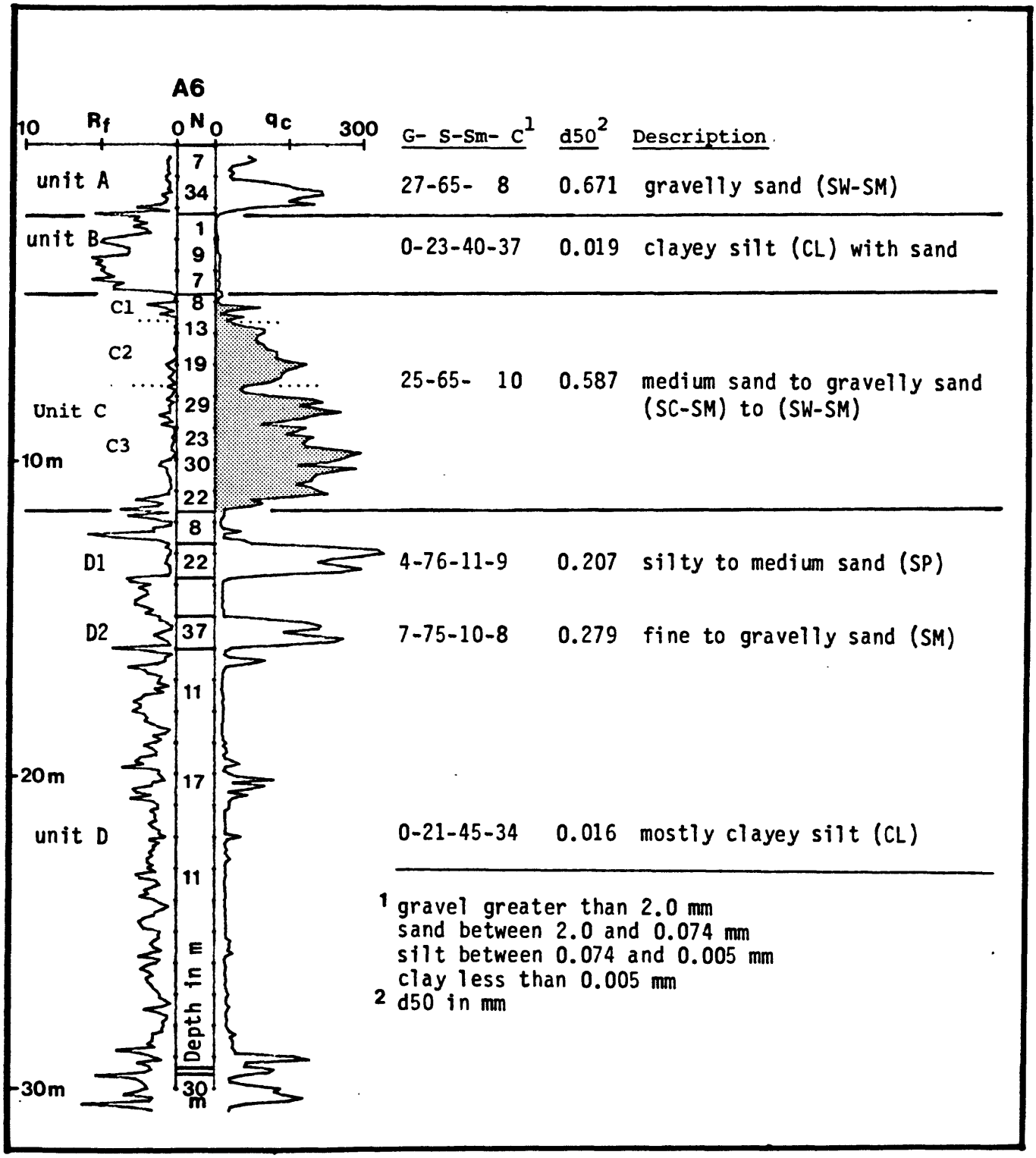

Figure 6. Log of sounding at A6. q_c is in kg/cm^2 , R_f is in percent, and N is in blow/ft. Grain size represent average value for entire unit.

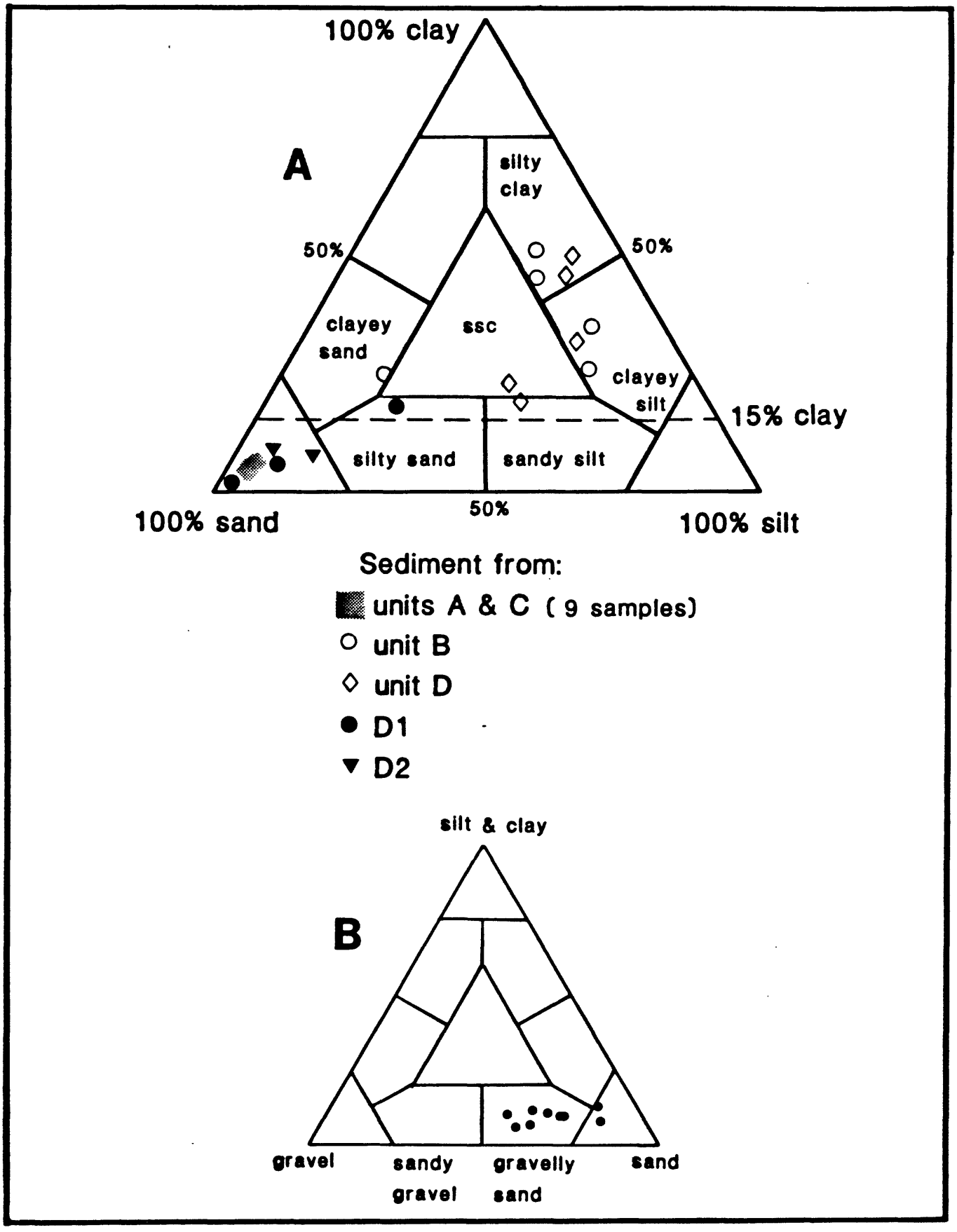

Figure 7. Ternary size diagram. All samples from A6 are show in A. The nine gravelly samples from units A and C are shown in B.

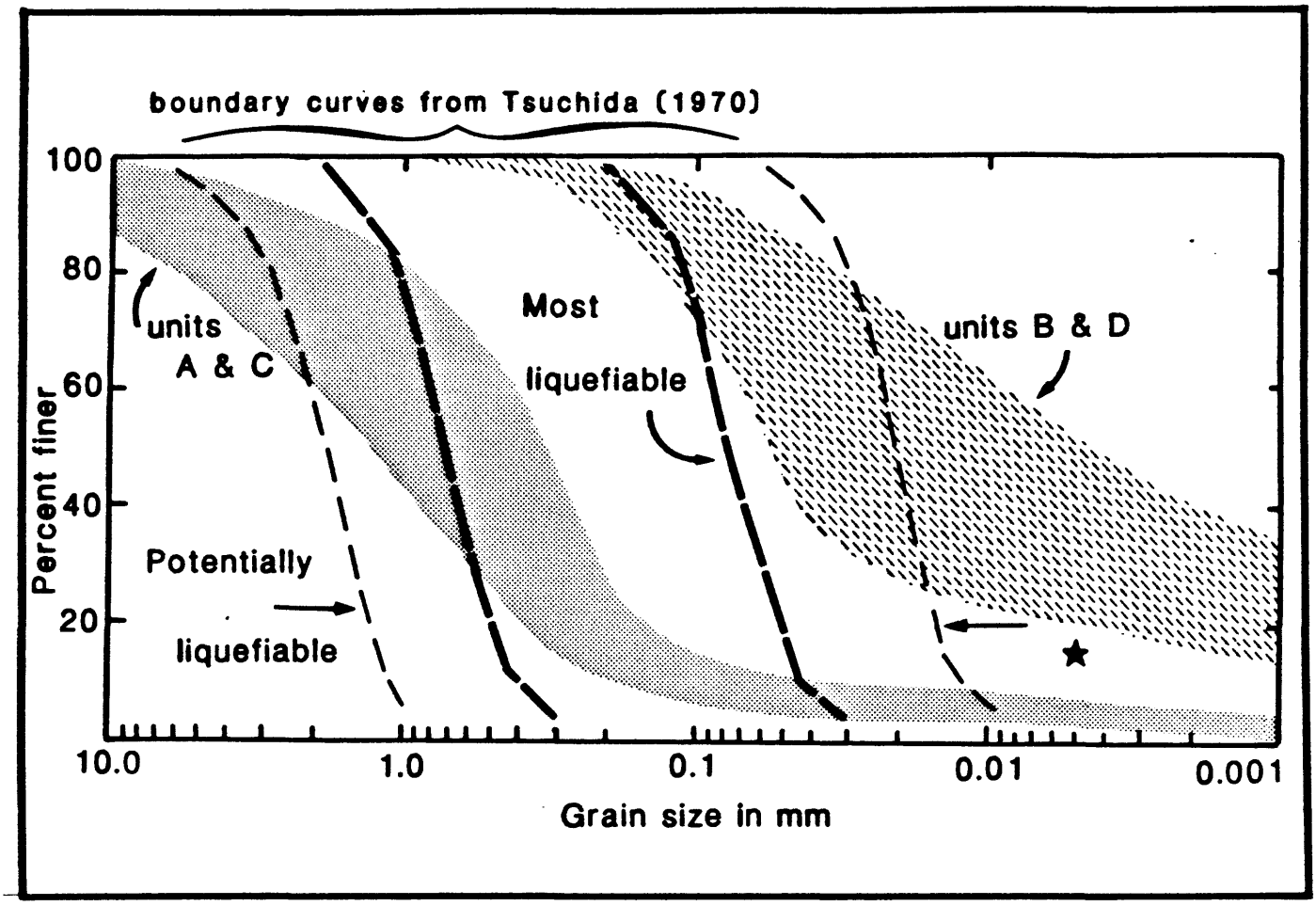

Figure 8. Size distribution of sediment from A6 is compared with the boundary curves showing the range in grain size of most liquefiable and potentially liquefiable sediment (Tsuchida, 1970). The star represents the 15% clay (0.005mm) limit used by Seed and others (1985) to determine vulnerability to liquefaction, curves above the star are not vulnerable to liquefaction. Four of five curves from subunits D1 and D2 are below the star.

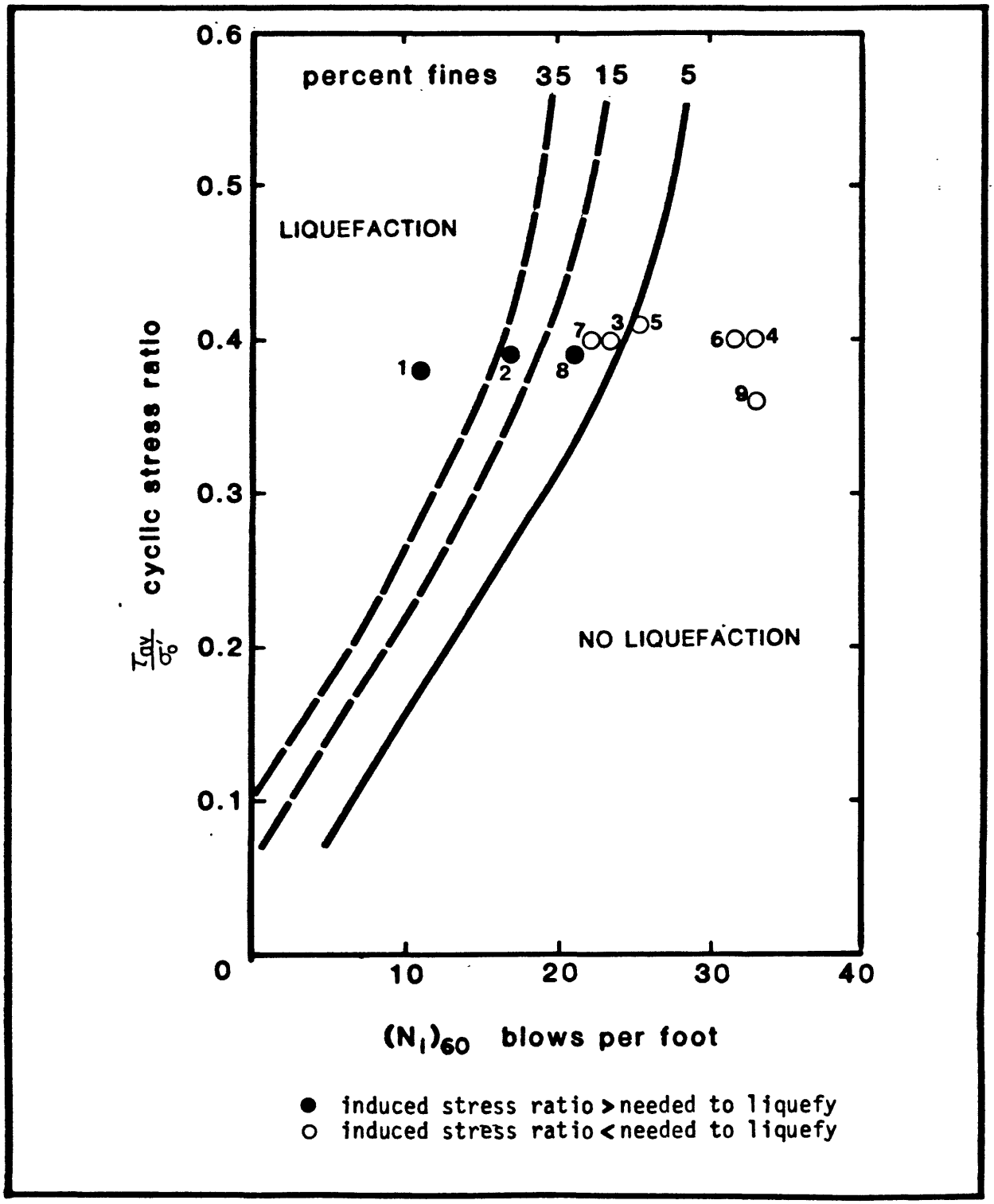

Figure 9. Relations between induced stress ratio, stress ratio needed to liquefy and corrected blow counts for a magnitude 5.6 earthquake. Depending on fine content the curves separate liquefaction on the left side, from no liquefaction on the right side (modified from Seed and others, 1985). Plotted points are identified in table 1. $(N_1)_{60}$ = N * Cn * 1.13, where N = blow/ft, Cn = factor to normalize to 1 kg/cm^2, and 1.13 = hammer energy correction. τ_{av} = average cyclic shear stress and σ'_v = vertical effective stress.

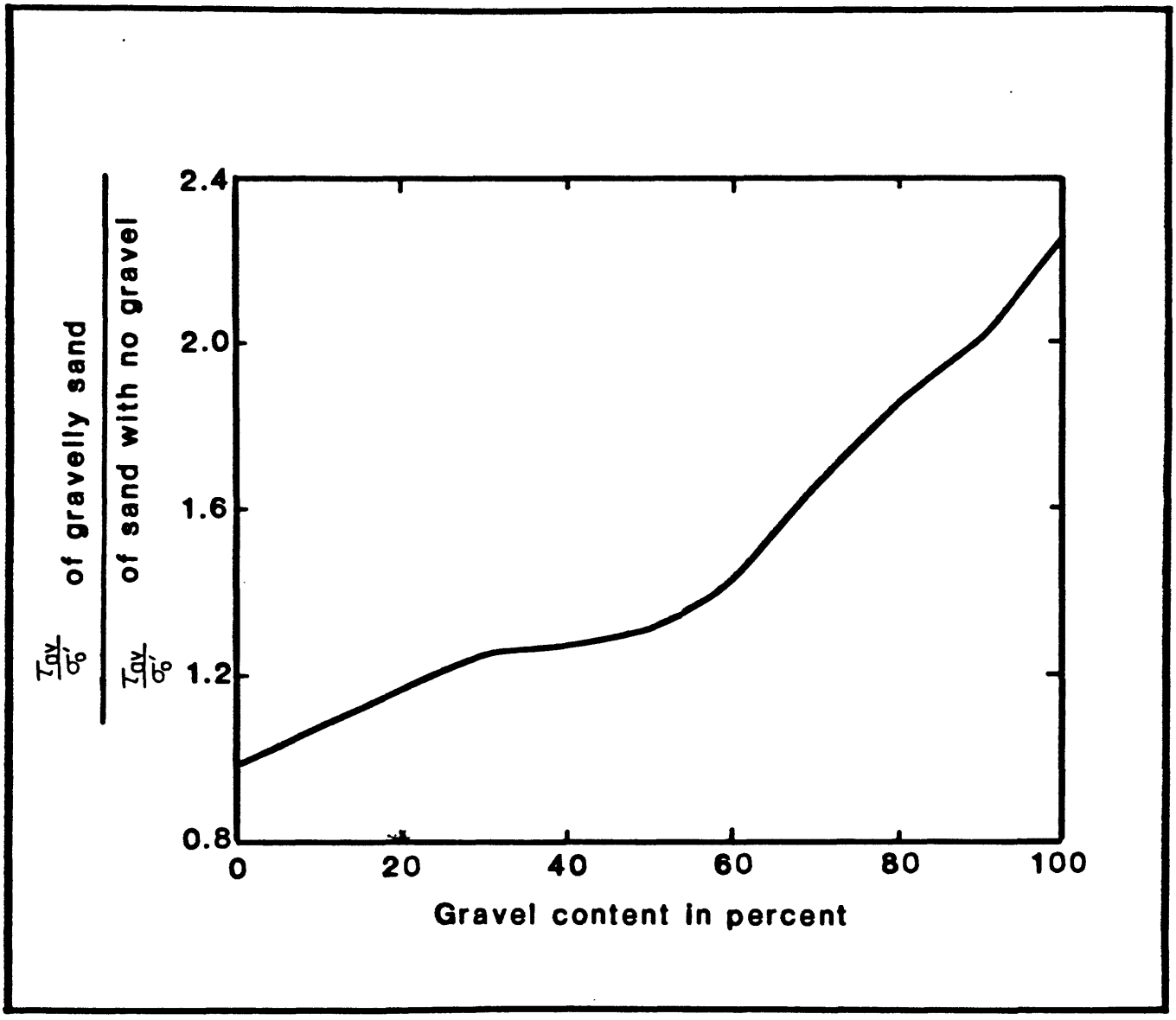

Figure 10. The ratio between stress ratio of gravelly sand and stress ratio of sand with no gravel is used with the gravel content to determine the correction factor for gravelly sand (Ishihara, 1985).

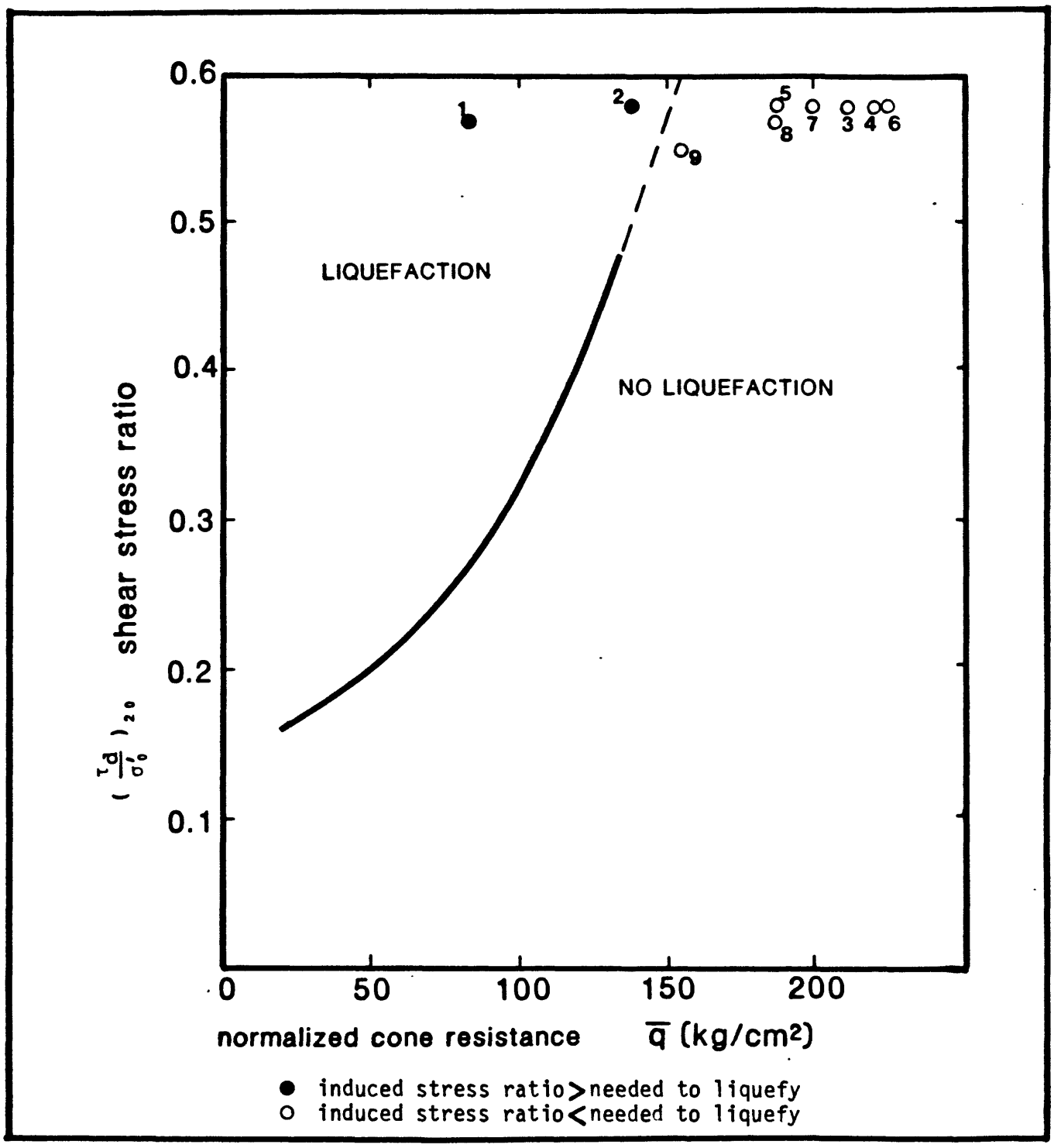

Figure 11. Boundary curve separates no liquefaction from liquefaction based on CPT (Ishihara, 1985). Plotted points are identified in table 2. $q = qc * Cn + 26(\log_{10}C)$, where q = normalized penetration resistance, q_c = tip resistance in kg/cm^2, C_n = normaliztion factor to 1 kg/cm^2, and C = is fines content, in percent.
$(\frac{\tau_d}{\sigma'_o})_{20}$ = cyclic-stress ratio required to cause initial liquefaction in 20 cycles of shear stress (independent of magnitude)

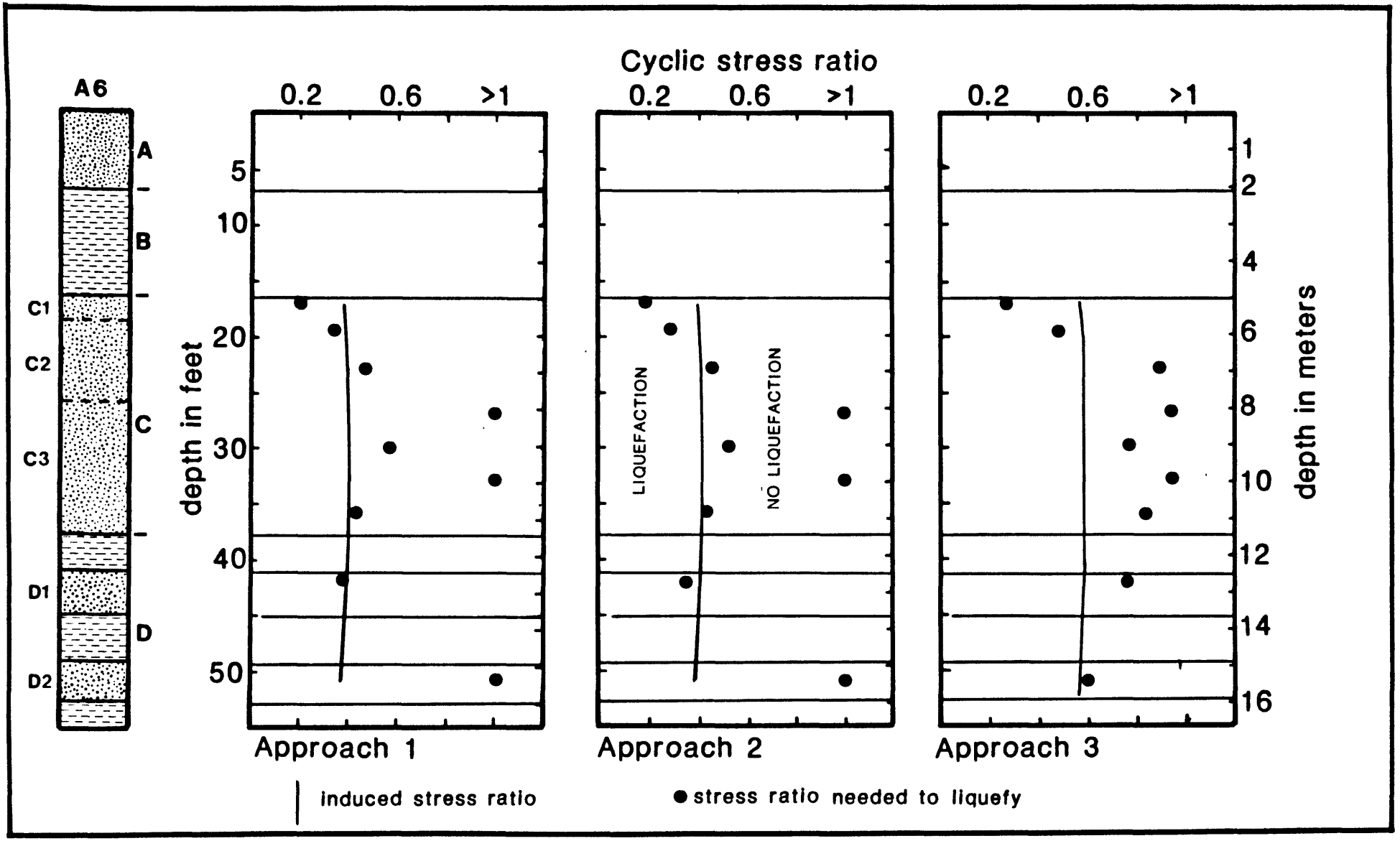

Figure 12. The relation between induced stress ratio (line) and stress ratio needed to liquefy (dots) is shown for the three approaches used in the investigation.

Table 1. SPT data to calculate liquefaction resistance.

depth (m)	N	fine content	gravel content	$(N_1)_{60}$	induced stress ratio	stress ratio needed to liquefy for fine	for gravel	#
		in percent						
5.2	8	8	12	11.0	0.38	0.20	0.19	1
5.9	13	13	10	17.0	0.38	0.34	0.29	2
7.0	19	11	26	23.1	0.40	0.47	0.46	3
8.2	29	9	38	33.1	0.40	**	**	4
9.1	23	11	30	25.3	0.41	0.57	0.53	5
10.1	30	6	37	31.8	0.40	**	**	6
11.0	22	10	22	22.5	0.40	0.43	0.43	7
12.8	22	9	6	21.3	0.39	0.38	0.35	8
15.5	37	18	7	33.2	0.36	**	**	9

** at this $(N_1)_{60}$ there is no stress ratio that will liquefy the deposit. $(N_1)_{60} = N * C_n * 1.13$, where N = blow/ft, C_n = correction to normalize to 1 ton/ft^2, and 1.13 energy correction factor for safety hammer. Index numbers in last column can be used to identify plotted points in fig. 9.

Table 2. CPT data to calculate liquefaction resistance.

Depth (m)	q_c	fine content percent	q_c'*	induced stress ratio	stress ratio needed to liquefy	#
5.2	44	8	83	0.57	0.27	1
6.1	87	13	137	0.58	0.49	2
7.0	161	11	210	0.58	0.89	3
8.2	195	9	220	0.58	0.94	4
9.1	167	11	186	0.58	0.76	5
10.1	222	6	221	0.58	0.94	6
11.0	201	10	198	0.58	0.82	7
12.8	211	9	185	0.57	0.75	8
15.5	178	18	154	0.55	0.58	9

* $qc' = Cn * qc + 26(\log C)$ where q_c is CPT tip resistance in kg/cm^2, Cn is factor to correct to 1 ton/ft^2, and C = fine content in percent. Index numbers in last column can be used to identify plotted points in fig. 11.

Table 3. Factor of safety (FS) of subunits at CPT A6.

Depth (m)	Subunit	Approach I	Approach II	Approach III	Liquefaction
5.2	C1	0.5	0.5	0.4	yes
5.9	C2	0.9	0.7	0.6	yes
7.0	C2	1.2	1.2	1.3	no
8.2	C3	>2.0	>2.0	1.4	no
9.1	C3	1.4	1.3	1.1	no
10.1	C3	>2.0	>2.0	1.4	no
11.0	C3	1.1	1.1	1.2	no
12.8	D1	1.0	0.9	1.1	probably not
15.5	D2	>2.0	>2.0	1.1	no

Approach I is the Seed and others (1985) SPT-based method which considers the effect of silt but ignores the effect of gravel on liquefaction resistance. Approach II is the Seed and others (1985) methods as modified by Ishihara (1985) to include the effect of gravel. Approach III is the Ishihara (1985) CPT-based method that includes the effect of silt on liquefaction resistance. A factor of safety less than one indicates that the cyclic-stress ratio induced by the earthquake is greater than the cyclic-stress ration needed to liquefy the deposit.

Appendix A. Logs of exploratory hand-augered holes

PC-1 Depth to water from land surface datum (LSD) = 0.72 m. PC-1 was augered in the bank of Cholame Creek. The land surface datum was about 2 m below the prevailing ground elevation.

Depth, m From	To	Description
0.00	0.74	sandy silt
0.74	1.12	dark olive gray, loose sand, organics
1.12	1.30	
1.30	1.52	black, dilatant silt
1.91	2.01	
2.01	2.11	dark olive gray, hard, medium stiff, silty clay
2.11	2.21	plastic organic-rich silty clay
2.21	2.39	
2.39	2.51	
2.51	2.67	coarse sand and olive gray stiff silty clay
2.67	2.82	

PC-2 Depth to water from LSD greater than 1.96 m

Depth, m From	To	Description
0.00	0.30	plastic clayey silt at top, grading downward to coarser and less plastic silt
0.30	0.38	silt, very dry
0.41	0.56	brown clayey silt, dry
0.56	0.74	gypsiferous clayey silt, dry
0.74	0.89	gypsiferous, stiff clayey silt, dry
0.89	1.04	silt, dry
1.04	1.19	sandy silt
1.19	1.35	sandy silt
1.50	1.65	stiff clayey silt
1.65	1.80	olive brown, clayey silt, dry
1.80	1.96	gypsiferous olive brown, very stiff, clayey silt

Appendix A. Logs of exploratory hand-augered holes.

PC-3 Depth to water from LSD = 0.64 m

Depth, m From	To	Description
0.00	1.52	rooty sand with clay and silt
1.88	2.03	sandy silt to silt
2.13	2.29	clayey silt
2.36	2.51	medium stiff clayey silt
2.57	2.72	stiff silty clay
2.74	2.90	clayey sand
2.90	2.97	sandy sediment, hard to auger

PC-4 Depth to water from LSD = 1.72 m

Depth, m From	To	Description
1.47	2.29	black silt
2.29	2.51	coarse, poorly sorted sand
2.51	2.64	coarse sand and brown stiff clay
2.64	2.84	brown stiff clay
2.84	2.95	stiff clayey silt

Appendix B. Seismic Refraction Interpretations

Site	Layer 1		Layer 2		Depth to top of layer 2 (m)
	V_n m/sec	V_s	V_n m/sec	V_s	
SR-1	375	350	1400	1650	1.7
SR-2	352	333	1325	1325	5.8
SR-3	350	350	1250	1325	0.9
SR-4	365	340	1420	1700	4.5
SR-5	340	348	1690	1490	6.0
SR-6	340	350	1680	1470	5.6
SR-7	396	360	1280	1630	7.3
SR-8	348	358	1650	1320	5.3
SR-9	342	344	1520	1520	6.0

Notes:

1. All lines were 65 m long. A hammer was used for energy source.
2. V_n is apparent velocity with source on south end of line; V_s is apparent velocity with source on north end of line.

Appendix C. Water level data

C1. Water levels in hand augered holes: June 5-7, 1985

Site	Depth to water, m	Approximate elevation of water surface, m
SR-1	1.7	354.0
SR-2	1.3	353.8
SR-3	0.8	357.0
SR-4	1.0	357.5
SR-5	1.2	356.9
SR-6	1.4	351.3
SR-7	2.1	357.6
SR-8	3.3	345.7
SR-9	3.4	345.6

C2. Water level measurements in piezometers near CPT A6

Date	Depth to water from land surface, m	
	Shallow piezometer[1]	Deep piezometer[2]
07/11/95	1.70	1.68
11/25/85	-	1.82
12/21/85	1.47	1.46
03/25/86	0.58	0.59
05/08/86	0.67	0.69

[1] Screened from 2.13 to 3.05 m below land surface

[2] Screened from 10.22 to 10.72 m below land surface

Appendix D. Sediment properties, A5

Depth[1] (m)	grain size[2] G -S -SM-C	d50[3] mm	Cu[4]	Atterberg limits[5] LL	PI	w/c	N	Description
1.1	42-49- 9- 0	1.30	22				12	gravelly sand (SP-SM)
2.4	0-14-40-46	0.006		47	25	27	2	silty clay (CL)
3.5	0- 7-41-52	0.005		45	24	27	6	silty clay (CL)
5.9	4-67-17-12	0.148	95				5	silty sand (SC-SM)
6.9	32-58- 10	0.550	13				9	gravelly sand (SP-SM)
7.9	51-42- 7	2.11	19				22	sandy gravel (SP-SM)
8.7t	62-32- 6	4.70	38					sandy gravel (GP-GM)
8.7b	5-84- 4- 7	0.448	12				16	medium sand (SP-SM)
10.5	0-55-33-12	0.086					21	silty sand (SC-SM)
12.5	3-85- 4- 8	0.249	9				26	fine sand (SC-SM)

1 depth is to midpoint of bottom 12 inches of penetration of SPT sample, example, 2.5 to 4 ft is recorded as 1.1 m (3.5 ft). In cases where more than one grain size test was conducted on a SPT sample the letters t, m, and b show the position of the grain size test within the SPT sample

2 gravel (G) size greater than 2.0mm (in percent).
sand (S) size between 2.0 and 0.075mm (in percent).
silt (SM) size between 0.075 and 0.005mm (in percent).
clay (C) size less than 0.005mm (in percent).

3 d50 is median grain size in mm, grain size at the 50th percentile.

4 Cu is coefficient of uniformity (d60/d10) grain size at 60th percentile divided by the grain size at the 10th percentile

5 Atterberg limits, LL is the liquid limit, PI is the plasticity index, and w/c is the natural water content (in percent).

Sediment properties, A6-deep

Depth (m)	grain size G -S -SM-C	d50 mm	Cu	Atterberg limits LL	PI	w/c	N	Description
0.6	21-69- 10	0.450	9				7	gravelly sand (SW-SM)
1.2	33-60- 7	1.0	10				34	gravelly sand (SW-SM)
2.4	4-52-19-25	0.123		31	13	31	1	clayey sand (SC)
3.4	0-18-37-45	0.008		38	18	26	9	silty clay (CL)
4.3t	0-15-34-51	0.005		49	26	30		silty clay (CL)
4.3b	0-13-52-35	0.017		41	19	30	7	clayey silt (CL)
5.2t	0-18-56-26	0.030		35	13	32		clayey silt (CL)
5.2b	12-80- 8	0.440	5				8	medium sand (SP-SM)
6.1	10-77- 6- 7	0.316	16				25*	medium sand (SC-SM)
7.0	26-63- 11	0.360	9				19	gravelly sand (SW-SM)
8.2	38-52- 10	1.10	22				29	gravelly sand (SW-SM)
9.1	30-59- 6- 5	0.730	20				23	gravelly sand (SW-SM)
10.1	37-57- 6	1.22	10				30	gravelly sand (SP-SM)
11.0	22-68- 10	0.490	8				22	gravelly sand (SW-SM)
11.9	0-17-51-32	0.017		34	12	26	8	clayey silt (CL)
12.8t	1-57-24-18	0.098						silty sand (SM)
12.8m	8-88- 4	0.460	3					medium sand (SP)
12.8b	4-82- 8- 6	0.197	5				22	fine sand (SM)
15.5t	12-73- 6- 9	0.440	71					gravelly sand (SM)
15.5b	2-76-14- 8	0.177	9				37	fine sand (SM)
17.7	0- 9-41-50	0.005		50	25	26	11	silty clay (CL)
20.4t	0-34-47-19	0.056		28	6			silty sand (CL-ML)
20.4b	0-34-43-23	0.041		29	9	21	17	clayey-sandy silt(CL)
23.2	0-12-42-46	0.006		46	22	27	11	clayey silt (CL)

[1] two separate SPT holes were made at CPT A6, except for the blow count (25) at 6.1 m data from A6-deep are used in the liquefaction resistance analysis.

* this blow count is not valid due to excess sand in the sampler, the blow count (13) from A6-shallow (depth = 5.9 m) is used in place of N = 25

Sediment properties, A6-shallow

Depth (m)	grain size G -S -SM-C	d50 mm	Cu	Atterberg limits LL	PI	w/c	N	Description
0.6	14-77- 9	0.345	7				6	medium sand (SW-SM)
1.4	43-51- 6	1.44	14				22	gravelly sand (SP-SM)
2.4	2-22-39-37	0.013		40	18	31	2	sandy-clayey silt(CL)
3.4t	0-23-38-39	0.013		40	19	27		sandy-silty clay (CL)
3.4b	0-10-34-56	0.003		49	25	28	4	silty clay (CL)
4.3	0-26-34-40	0.012		41	18	25	6	sandy-clayey silt(CL)
5.2t	0-10-53-37	0.014		40	18	35		clayey silt (CL)
5.2b	13-71- 7- 9	0.294	44				8	gravelly sand (SM)
5.9	0-90- 10	0.260	4				13	medium sand (SP-SM)
7.0	10-81- 9	0.280	4				24	medium sand (SP-SM)
11.0	15-75- 10	0.390	7				60*	medium sand (SW-SM)

* this blow count is not valid due to excess sand in sampler

Sediment properties, A7

Depth (m)	grain size G -S -SM-C	d50 mm	Cu	Atterberg limits LL	PI	w/c	N	Description
1.2	0-38-47-15	0.054	54			30	3	sandy silt (ML)
2.6	0-12-52-36	0.011		36	13	36	1	clayey silt (CL)
4.1t	0- 7-41-52	0.004		55	30	36		silty clay (CH)
4.1b	0- 5-48-47	0.006		54	26	35	9	clayey silt (CH)
5.3	0-59-29-12	0.097	51				8	silty sand (SM)
7.2	22-70- 8	0.550	7				29	gravelly sand (SW-SM)
8.2	0-66-22-12	0.130	72				21	silty sand (SC-SM)
9.0	14-81- 5	0.560	4				19	coarse sand (SP-SM)
9.9	17-78- 5	0.600	6				22	coarse sand (SW-SM)
11.1	0-85- 9- 6	0.208	5				34	fine sand (SM)
12.2	0- 4-50-46	0.006		47	23	31	9	clayey silt (CL)
413.1	9-79- 7- 5	0.325	7				22	medium sand (SP-SM)

Sediment properties, C2

Depth (m)	grain size G -S -SM-S	d50 mm	Cu	Atterberg limits LL	PI	w/c	N	Description
0.6	36-58- 6	0.960	11				13	gravelly sand (SP-SM)
1.4	36-40-16- 8	0.730	97				1	sandy gravel (SM)
2.4t	0-34-42-24	0.045		29	11	26		clayey-sandy silt(CL)
2.4b	0-17-43-40	0.010		39	20	29	4	clayey silt (CL)
3.4t	0-36-37-27	0.039		31	11	28		clayey-sandy silt(CL)
3.4b	0-32-40-28	0.040		33	14	25	3	clayey-sandy silt(CL)
4.9	2-85- 7- 6	0.201	5				8	fine sand (SM)
5.8	22-68- 10	0.415	7				20	gravelly sand (SW-SM)
6.7	56-36- 8	4.0	96				23	sandy gravel (GP-GM)
7.6	31-63- 6	0.750	9				22	gravelly sand (SP-SM)
9.1	0-28-54-18	0.041				24	13	sandy silt (ML)

Sediment properties, C3

Depth (m)	grain size G -S -SM-C	d50 mm	Cu	Atterberg limits LL	PI	w/c	N	Description
0.8	46-47- 7	1.43	22				15	sandy gravel (SP-SM)
2.6t	1-26-43-30	0.028		43	21	36		sandy-clayey silt(CL)
2.6b	0-20-41-30	0.015		43	21	27	2	sandy-clayey silt(CL)
4.3t	1-18-41-40	0.011		47	25	28		clayey silt (CL)
4.3b	0-25-35-40	0.013		37	17	27	7	sandy-silty clay (CL)
5.2	1-72-15-12	0.154	55				7	fine sand (SM)
6.1	18-73- 9	0.305	4				18	gravelly sand (SP-SM)
7.2	18-72- 10	0.420	7				19	gravelly sand (SW-SM)
8.1	36-59- 5	0.870	6				13	gravelly sand (SP)
9.4	18-70- 6- 6	0.530	15				33	gravelly sand (SW-SM)
10.2	0-15-61-24	0.028		31	7	30	10	clayey silt (ML)